LBL-13336

Lawrence Berkeley Laboratory
UNIVERSITY OF CALIFORNIA

Materials & Molecular
Research Division

Presented at the International Conference on Solid-Solid Phase Transformations, Pittsburgh, PA, August 9-14, 1981

SOLID STATE PHASE TRANSFORMATION MECHANISMS

K.H. Westmacott, U. Dahmen, A. Pelton, and M.J. Witcomb

September 1981

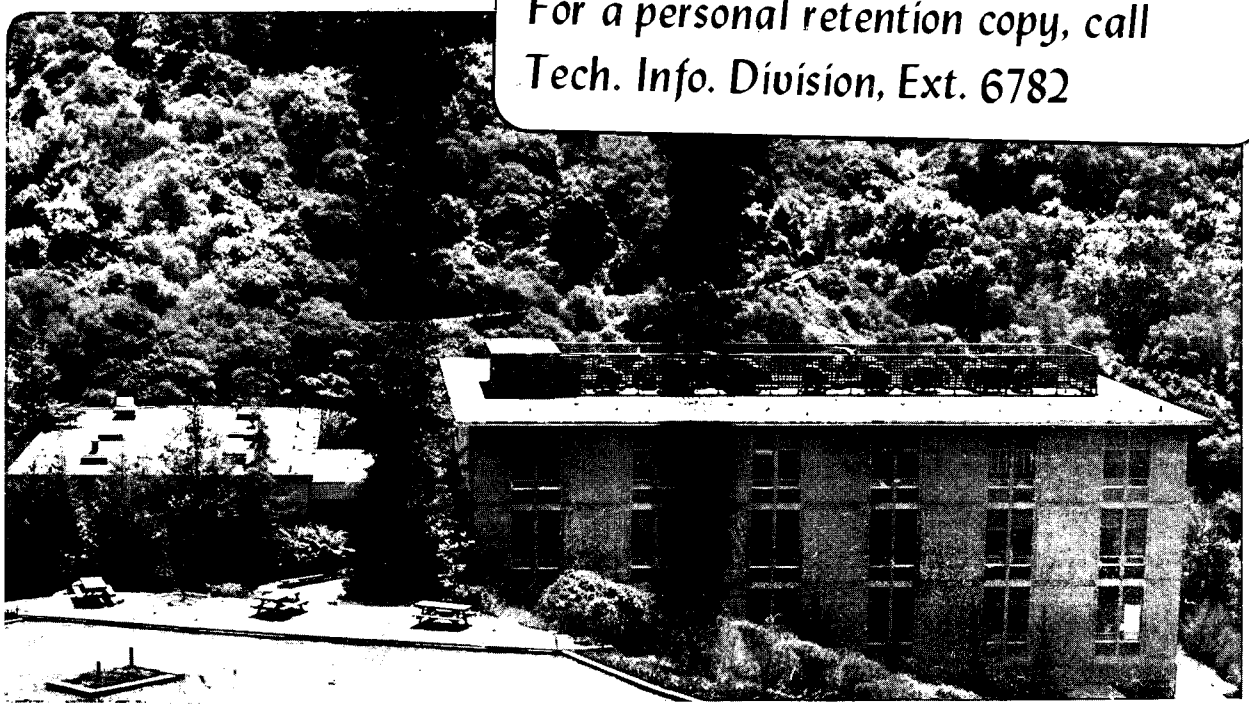

Prepared for the U.S. Department of Energy under Contract W-7405-ENG-48

DISCLAIMER

SOLID STATE PHASE TRANSFORMATION MECHANISMS

K. H. Westmacott, U. Dahmen, A. Pelton and M. J. Witcomb*

Materials and Molecular Research Division
Lawrence Berkeley Laboratory
University of California
Berkeley, CA 94720

SUMMARY

In many solid state transformations a new phase with a different crystal structure (the product) forms in the matrix of the old structure (the parent). With rare exceptions, there is a volume difference between the new and old phase which results in the development of lattice strains in both parent and product especially if the transformation occurs under non-equilibrium conditions. It is not surprising therefore that both the nucleation and growth of the new phase should have a close connection with crystal lattice defects since such defects also perturb the lattice. Nevertheless, very few systematic studies of the structural role of crystal defects in phase transformations have been attempted.

This report combines a series of papers presented recently at International Conferences which explores this inter-relationship in a number of alloy systems. The powerful direct observational techniques of transmission electron microscopy are used to study precipitation in both simple model systems and more complex alloys of practical importance. The main goal is to elucidate the underlying mechanisms operating during a precipitation reaction and improve our understanding of the role of lattice defects, and to develop a more unified picture

*Electron Microscope Unit, University of Witwatersrand, Johannesburg, South Africa

of the process.

It is shown that lattice defects, particularly vacancies and dislocations, can indeed adopt the necessary diversity of configurational arrangements to facilitate the formation, growth and accommodation of disparate phases.

In Paper I the results of a detailed study of a model system Pt(C) are summarized. The results of this work, together with those from a comprehensive study of Ta(C), have emphasized the importance of solute atom/vacancy association and co-precipitation. Moreover, the structural role of vacancies and their relationship to crystallography in the establishment of a new phase has been clarified.

Paper II presents the results of observations made on commercial austenitic and ferritic steels which show that the concepts developed for simple systems can be applied successfully to complex alloys.

In Paper III the application of convergent beam electron diffraction to the determination of the structure of very small precipitates in Pt(C) is described.

Paper IV outlines the theoretical framework which is proving remarkably successful in describing the role of lattice defects in the establishment of orientation relationships, precipitate morphology, and changes that occur during growth, as well as the connection between different orientation relationships.

In Paper V a qualitative theory is advanced which takes into account the interplay between vacancies and solute atoms in the formation of precipitates and/or secondary defect structures. The predictions of the model for extreme conditions where one of the many factors

involved dominates is in good agreement with experimental observations.

Together, this series demonstrates new links between previously disparate aspects of phase transformations and provides a more unified approach to the problem. While a great deal of experimental work is required to clarify many facets of the problem, the value of the present approach is already clearly evident.

PAPER 1

The solubility of carbon in platinum is about 0.1 a/o at the melting point and vanishingly small at ambient temperatures[1]. Recent studies have shown that in carbon bearing Pt alloys, an intermediate carbide phase precipitates in the presence of quenched-in vacancies[2]. The structure in as-quenched samples is particularly simple and may be explained as the co-precipitation of tightly bound carbon atoms and vacancies in a monolayer on {001} matrix planes[3]. During subsequent ageing in the temperature range 400-530°C, further structural transitions occur as the precipitate density decreases and the diameter and thickness increase. Because of the low volume fraction of precipitates, the sequential changes in morphology and structure may be readily followed by electron microscopy. Consequently, a detailed study[4], part of which is reported here, has been carried out on this model system and new insights obtained on precipitate nucleation and growth mechanisms.

Results

Platinum foils containing ∿800 at.ppm (0.005wt%) of carbon were heated and quenched in an all-metal bakeable high vacuum system with an ultimate vacuum of <1μPa (10^{-8} torr) to maintain the material purity. Because of the experimental uncertainties in measurements of carbon at these low levels and the paucity of accurate solubility data, indirect evidence was used to infer the presence and amounts of carbon in the Pt[4].

The series of micrographs shown in Figure 1 illustrate the evolution of the precipitate structure during post-quench ageing treatments. A detailed contrast analysis[3] of the as-quenched defects (seen in Figure 1(a)) has shown behavior that is consistent with collapsed

discs of vacancies and carbon atoms on {001} planes. The resulting faulted dislocation loop (designated α) is intrinsic (vacancy-type) and has a Burgers vector and fault displacement vector of $\sim 0.3a[001]$.

After ageing at 400°C for 24 hours, two types of precipitate ($\alpha + \alpha'$) are observed due to growth and thickening of some plates at the expense of others (see Figure 1(b)). The emerging α' precipitates also lie on {001} planes but they may be readily differentiated from the remaining 0.3{001} α plates by their larger size and different contrast behavior. A full analysis has shown that the α' defects are also of vacancy type but have Burgers and displacement vectors of a/2<001>. Other more complex defects are also found (e.g. at A) and a contrast analysis of these indicated that they are shrinking α' defects. This multiplicity of defects was observed throughout the foils and may be explained by a local time-dependent variation in the amounts of carbon in solid solution.

When the ageing temperature was increased to 500°C, a more uniform precipitate structure was found, as seen in Figure 1(c). The dislocation analysis of these defects showed mostly a/2<001> Burgers vectors, suggesting that they were also α' precipitates which had undergone a shape change from square to circular at the higher temperature. In some cases further thickening of the platelets had occurred to form α'' (e.g. at B) which were analysed as having a <001> vacancy-type strain fields.

Finally, after annealing foils in the temperature range 515° to 550°C, the density of α' precipitates decreased markedly as the size and complexity increased further. Most of the remaining precipitate plates were grouped together in linear arrays suggesting sympathetic re-nucleation or

association with a lattice dislocation (see Figure 1(d)). Some of the precipitates were changing further by the passage of partial dislocations or ledges across the broad face. The size of the precipitates at this stage was sufficient to allow convergent beam electron diffraction patterns to be taken. An analysis of the observed superlattice spots and corresponding precipitate structure is in progress[4] and has shown the precipitate structure to be tetragonal with a c/a ratio of $\sim$1.5. Lattice fringe images taken of precipitates at this stage confirm that the platelets are semi-coherent since a missing fringe is observed at the end of the platelet (see arrows in Figure 2). Measurements of the fringe spacings suggest a thickness of about seven {002} lattice spacings.

Discussion

The terms defect structure and precipitate structure have deliberately been used interchangeably to emphasize the fact that the transition from the simple vacancy loop structure in the as-quenched material to the true precipitate structure after ageing is continuous and the events closely related. Indeed, the initial monolayer defect can be considered either as a solute-decorated imperfect dislocation loop or as a thin semi-coherent precipitate, and it is fruitful to develop this analogy.

As is well known, an intrinsically faulted region can be created on a {111} plane in the FCC lattice either by nucleating and expanding a loop of a/6<112> Shockley partial dislocation or by condensing and collapsing a disc of vacancies to form an a/3<111> Frank loop. If the intrinsic fault thus formed is instead regarded as at thin plate of HCP material and the formation process as a phase transformation, the concept of coherency recently discussed and clarified by Olsen and Cohen[5] becomes

graphically clear. Identical precipitate structures are formed by a homogeneous shear transformation, in which case it is bounded by a coherency dislocation (i.e. the Shockley partial), and by a heterogeneous transformation where it is bounded by a misfit dislocation (the Frank partial). The distinction between the two processes lies in whether lattice sites are conserved (the coherent case) or eliminated (the semi-coherent case). The structures are clearly related and the second structure can be derived from the first by the addition of a matrix anti-coherency dislocation, i.e. a perfect loop with Burgers vector a/2 <110>. These considerations form the basis for understanding the precipitation sequence observed in the present study since completely analogous loop and precipitate reactions can occur on the {001} FCC planes.

A simple model which is consistent with the observed structural changes is outlined in the remaining discussion.

The α platelets observed in the as-quenched alloys form by the co-precipitation and collapse of vacancy-carbon atom complexes on {001} planes. These defects may be compared to the GPI zones which form in Al-Cu alloys except that from the outset the plates in Pt(C) are semi-coherent. The monolayer α precipitate may be regarded as the first or transition unit cell of the carbide structure (Figure 3(a)). It thickens to α' by the condensation of a second layer of vacancies and carbon atoms (Figure 3(b)). The resulting intrinsic dislocation loop with fault vector 0.5a<001> confirmed by contrast analysis cannot be produced by a single layer defect in an FCC lattice. At this and later stages of the precipitate development, the dislocation and fault contrast is therefore a superposition of several displacements on successive atomic planes,

equivalent to Olson and Cohen's[5] coherency dislocations. This fact opens up a number of different possibilities for the growth or skrinkage of α' platelets. The simplest and most commonly observed is the growth by further addition of carbon and vacancies to form a four-layered α'' defect (Figure 3(c)). The growth sequence discussed so far involves vacancies at every stage, analogous to the formation of a layer of hexagonal material by condensation of successive Frank loops. However, as noted before, the same structure can also be produced by the propagation of shear loops analogous to Shockley partials. This has in fact been observed as shown by a contrast analysis in Figure 4. The shear component of the dislocation bounding the irregularly shaped precipitate is clearly visible in the {200} reflection, whereas the pure edge components in this and the other neighboring α' defects are invisible. The analysis of Figure 4 shows that the double layer precipitate is shrinking by the shear of one layer accompanied by the evaporation of the other layer of vacancies. Another possibility is a double shear mechanism involving two dislocations of the type $1/4\langle 201\rangle$. All three mechanisms are available for both shrinkage and growth of precipitates but so far shear components have only been observed in shrinking precipitates.

The nucleation and growth proposed for the Pt(C) system also occurs in other alloy systems where oversize phases precipitate, and further examples are reported elsewhere in the Proceedings.

ACKNOWLEDGEMENTS

This work was supported by the Director, Office of Energy Research, Office of Basic Energy Sciences, Materials Science Division of the U.S. Department of Energy under Contract No. W-7405-ENG-48, and a grant from

the Science Research Council of South Africa.

REFERENCES

1. E. Fromm, E. Gebhardt, eds., Gase and Kohlenstoff in Metallen, Springer, New York (1976), pp. 648-650.
2. M. J. Witcomb, U. Dahmen and K. H. Westmacott, Proceedings of the EMSSA Meeting, Pretoria (1981), in press.
3. K. H. Westmacott and M. I. Perez, J. Nucl. Mat. 83, 231 (1979).
4. K. H. Westmacott, M. J. Witcomb and U. Dahmen, to be published.
5. G. B. Olson and M. Cohen, Acta Met. 27, 1907 (1979).

FIGURE CAPTIONS

Fig. 1 (a) {001} single layer α precipitate in as-quenched Pt.

(b) $\alpha+\alpha'$ precipitates after aging 24 hours at 400°C (courtesy M. Perez)

(c) Circular double-layer precipitates (α') after aging 30 hrs. at 500°C. Four-layer precipitate at B.

(d) Linear arrays of circular α' precipitates after aging 1 hour at 515°C.

Fig. 2 Two-beam lattice fringe image showing missing fringe at the end of α' precipitate (arrows).

Fig. 3 Possible growth sequence in the transition from solid solution to α to α' to α'' precipitates.

Fig. 4 Contrast analysis of a shrinking α' precipitate (arrow) showing a shear component, visible in a) and invisible ($\underset{\sim}{g}\cdot\underset{\sim}{b} = 0$) in C) (micrographs by M. Perez).

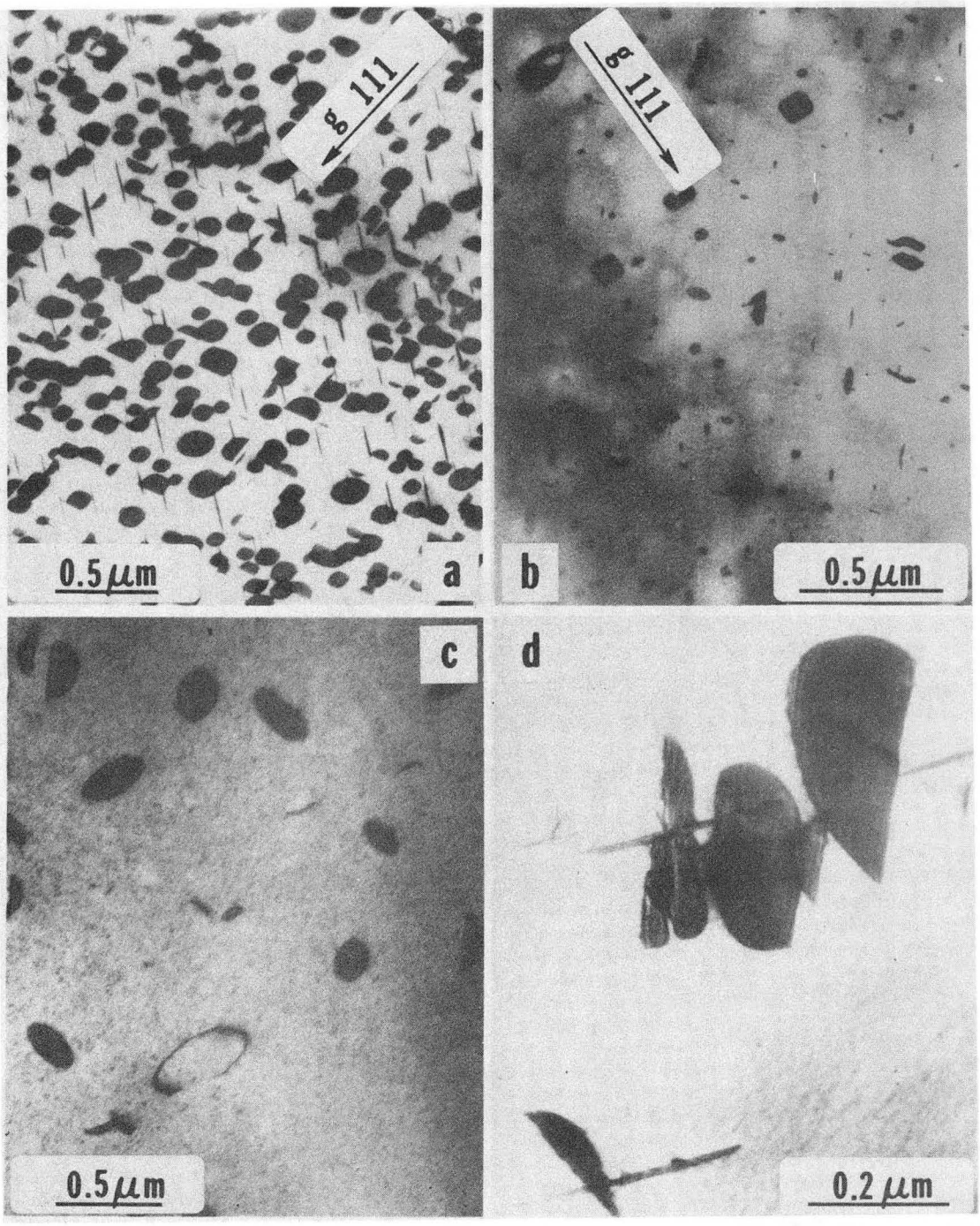

XBB 819-8427

Fig. 1

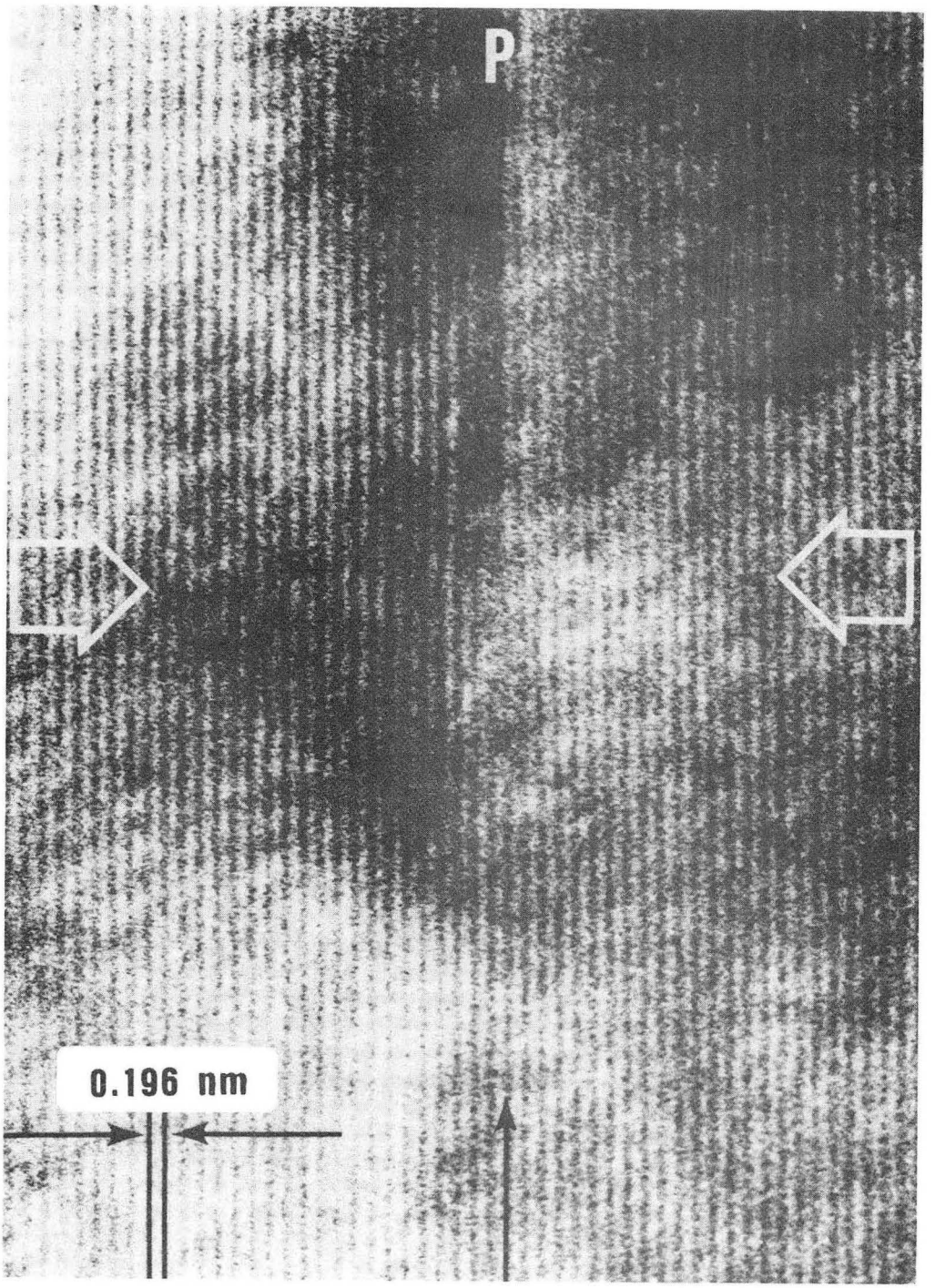

XBB 800-14620

Fig. 2

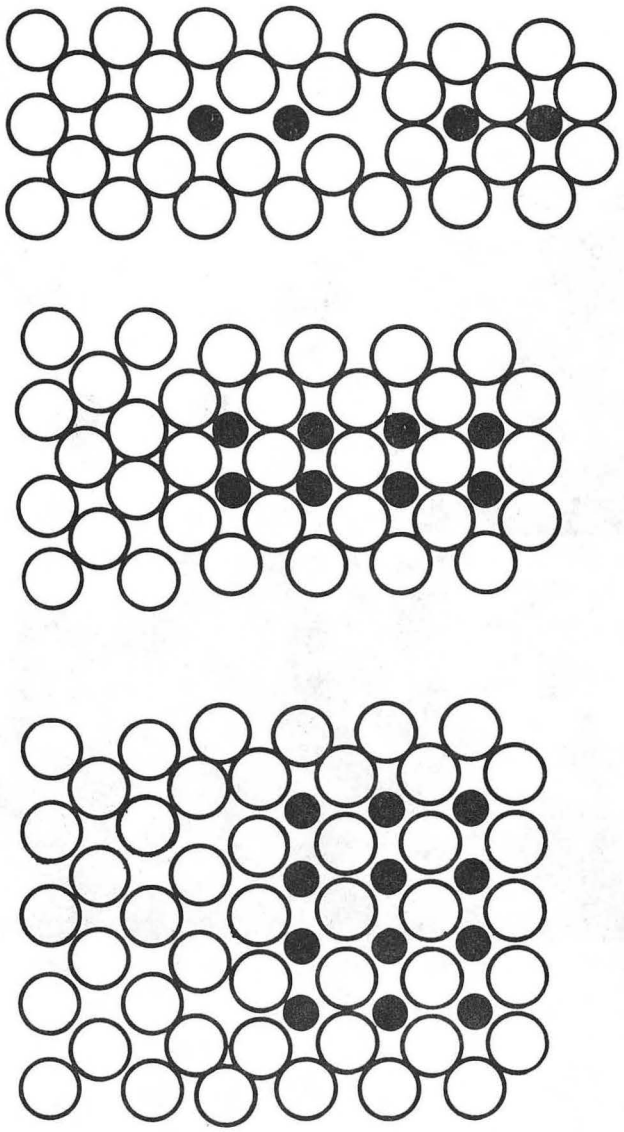

XBL 817-10912

Fig. 3

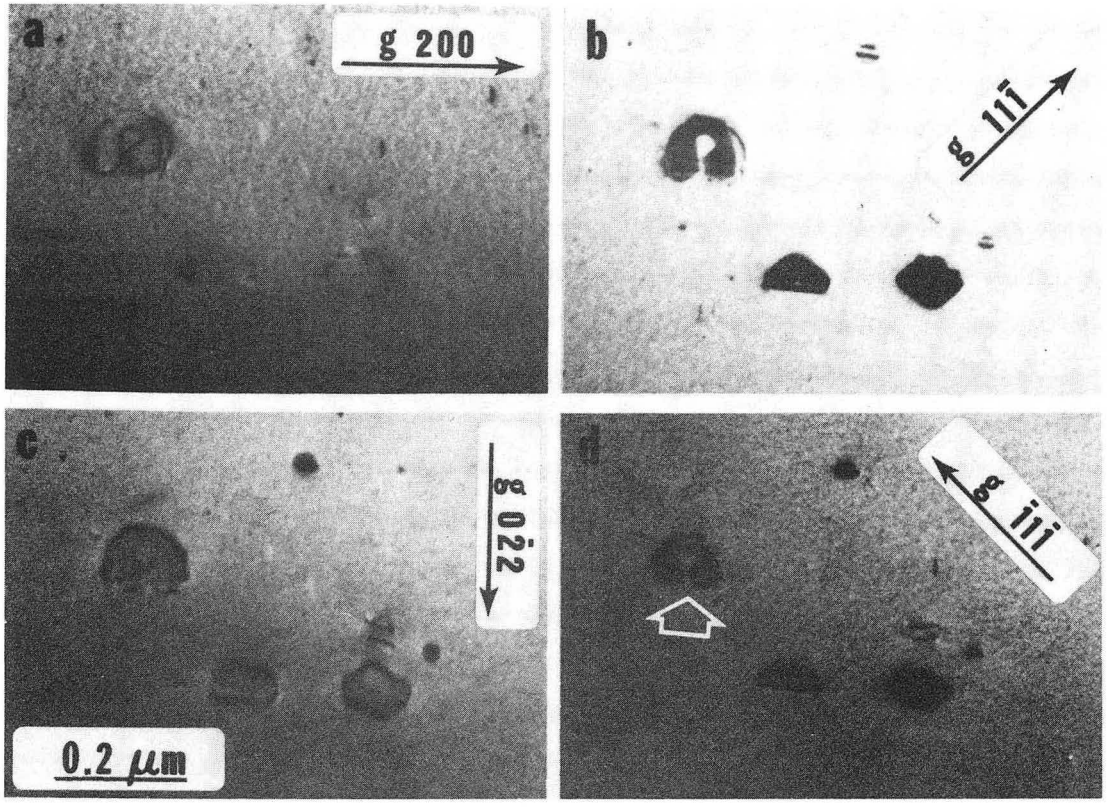

XBB 800-14621

Fig. 4

PAPER II

The interstitial phase precipitation reactions in ferritic Fe-Si (C) and austenitic Fe-Cr-Ni (C,P) alloys were studied via transmission electron microscopy. It was found that quenched-in vacancies play various roles in the nucleation and growth of these phases. In the ferritic steel, a single vacancy is capable of nucleating the incipient carbide phase. Growth of the carbide nucleus occurs by addition of migrating carbon atom to vacancy-carbon complexes. The formation of phosphides in the austenitic stainless steel is interpreted in terms of a vacancy-phosphorous co-precipitation model, whereas carbides in the austenite precipitate by a similar mechanism to that in the Fe-Si (C).

Introduction

Precipitation-hardenable ferritic and austenitic alloys containing interstitial solute have tremendous technological importance; as such, numerous investigations have been initiated to optimize the beneficial phase decomposition. For example, the low homologous temperature aging response of α-Fe doped with C or N has been studied extensively. The precipitation behavior of austenitic Fe-Cr-Ni steels alloyed with C, N or P also have received consideration attention. Although the phase transformation occurring during the process of quench-aging is exceedingly complex, these systems share many common microstructural characteristics. Examples of the microstructures observed after quench-aging these systems include:

- homogeneous dispersion of coherent or semicoherent plate-like precipitates,
- {100} habit planes with perpendicular displacement vectors,
- precipitate-free-zones near dislocations and grain boundaries,

- precipitate densities related to the excess vacancy concentrations.

These features traditionally have been explained solely in terms of the precipitation of supersaturated solute; although the involvement of excess vacancies has been recognized[1].

A companion paper in these proceedings[2] illustrates the salient features of vacancy-assisted precipitation of solute phases in various alloy systems. The paper develops a mechanistic approach to precipitation based on the accommodation of misfitting solute atoms and the structural and thermodynamic roles of vacancies. This approach has been successfully applied to carbide precipitation in fcc Pt(C)[3] and bcc Ta(C)[4]. It seems likely, therefore, that the model may be used to interpret the precipitation behavior in more complex systems. Thus, the purpose of the present paper is to compare the precipitation reactions in ferritic Fe-Si(C) and austenitic Fe-Cr-Ni(C,P) with each other, and with previous studies of similar alloys.

Experimental Procedures

The nominal compositions and thermal treatment schedules of the alloys used in this report are summarized in Table 1. Prior to thermal treatments, samples were cold rolled to $\sim$75μm, electropolished to clean the surfaces, and encapsulated in quartz tubes under a vacuum of $\lesssim 5 \times 10^{-6}$ torr. Specimens were quenched by breaking the capsules in ice water.

Experimental Results

Fe-Si(C)

Typical microstructures of precipitation in the ferrite phase of the Fe-Si(C) alloy aged at 25°C for 168hr is shown in Figure 1(a). Further

analysis shows that these incipient precipitates lie on {100} planes and have Burgers vectors of a/3<100>. The precipitate density is approximately 7 x 10^{15} cm^{-3}, and the particles are 15nm in diameter and 1.5nm thick. Attempts to identify the precipitates by electron diffraction were not successful; however, from the {100} habit planes, they were assumed to be epsilon carbide, or a precursory phase of epsilon carbide. Figure 1 (b) shows the structure of a sample aged at 25°C for 168hr and subsequently aged at 100°C for 1 hr. Note the precipitate-free zones near the grain boundaries and dislocations and that the dislocations are decorated with carbides.

Fe-Cr-Ni (C,P)

There are three distinct precipitation modes observed in the austenitic stainless steel aged at 500°C:

(i) β-{100} matrix precipitates which exhibit displacement fringes

(ii) β'-fine (∿5nm) matrix precipitates

(iii) β"-dislocation-nucleated precipitates

These three precipitate reactions will be reported in the following section.

(i) β-{100} matrix precipitates

Figure 2 shows high densities (∿$10^{15}cm^{-3}$) of the β-precipitates. These precipitates have coarsened only slightly with little change in density as the aging time at 500°C is increased from 10hrs (Figure 2(a)) to 100hrs (Figure 2(b)). A detailed analysis[5] of these precipitates showed that they are semi-coherent, intrinsic defects with {100} habit planes. In addition, displacement vectors $\underset{\sim}{R}$ and Burgers vector $\underset{\sim}{b}$ were determined to be a/3<100>.

(ii) β'-fine (∿5mn) matrix precipitates

The β' precipitates are also a product of the phase decomposition

occurring at 500°C. It was determined that the β' precipitates have spherically symmetric strain fields, and have an average density of 10^{16} cm^{-3}. Although no diffraction evidence was obtained from the precipitates, it is assumed that they are $M_{23}(C,P)_6$ based on studies of high carbon, high phosphorous steels[6].

(iii) β"-dislocation-nucleated precipitates

As seen in Figure 2(b), dislocations are potent nucleation sites for precipitation in the austenitic steel. It is thought that these particles are also $M_{23}(C,P)_6$. From weak-beam dark field stereo pairs and stereographic analyses, it was determined that: (1) The precipitates nucleate on dislocations with large edge components, especially on helical arrays. (2) The precipitates generally lie on {110} planes perpendicular to the dislocations' Burgers vectors.

The extent of this mode of precipitation is the major distinguishing feature between the samples aged at 500°C for 10hrs and 100hrs.

Discussion

It is instructive to compare the present observations with the results of previous studies on the relationship between quenched-in defects and precipitation in Fe-base alloys.

In Fe-Si(C) clear evidence is found that vacancies retained during quenching from the solution treatment temperature participate in the precipitation process, in agreement with the work of Vyhnal and Radcliffe[1] (V.R.) on Fe(C). In both systems the precipitation of ε carbide (or a precursor phase) is sensitive to both the quenching rate and subsequent aging temperature. Fast quenching followed by room temperature aging produces fine scale precipitation, whereas slow quenching or higher

temperature aging results in a coarse distribution of heterogeneously nucleated precipitates. V.R. have proposed a credible model to explain these effects. Carbide nucleation occurs because the interaction between the strain field of a vacancy-carbon atom complex and freely migrating interstitial carbon results in the formation of a critical sized vacancy/carbon cluster. In agreement with this model, the observed maximum density of precipitates ($10^{15}cm^{-3}$) can be equated to the excess vacancy concentration. In terms of the co-precipitation model of precipitate nucleation (outlined elsewhere in these Proceedings), this represents an extreme case in which the lattice perturbation associated with a single vacancy nucleates the new phase. However, a more detailed consideration of V.R.'s scheme suggests that the vacancies could participate in the growth as well as the nucleation of the precipitate.

The contrast of the β precipitates in the stainless steel is consistent with a structure consisting of a collapsed sheet of vacancies stabilizing a layer of phosphorous atoms. This particular type of defect, with $\underset{\sim}{b} = \underset{\sim}{R} \sim a/3\langle 100\rangle$ has been reported only once before in a fcc material, namely in Pt(C)[3]. Rowcliffe et al.[7,8] previously investigated the precipitation reactions in this phosphorous containing alloy; two major differences were found with the present study: First, Rowcliffe[7,8] also observed {100} intrinsic defects in samples directly quenched from 1100°C to 500°C and aged up to 50 hrs. However, in the absence of any detectable displacement fringes, they deduced that $\underset{\sim}{b} \sim na\langle 100\rangle$. The $a/3\langle 100\rangle$ precipitates could, therefore, be a precursor to the $a\langle 100\rangle$ structures; this is in accord with the precipitation sequence in Pt(C)[3]. A second difference is the absence of voids in the present work. This is attributed to the elimination

of oxygen pickup by using vacuum quenching. In the absence of oxygen and void formation, all the excess vacancies are available for precipitate formation by the co-precipitation mechanism. However, the observation of the two types of matrix precipitate, β and β', suggests that the vacancies have partitioned between carbon and phosphorous solute atoms. The estimated vacancy concentration incorporated in the β precipitates, assuming monolayer co-precipitation, is 10^{-5} in agreement with calculated retained vacancy concentrations assuming no losses during the quench. Thus, the observations may be explained if β phosphorous-rich precipitates form by the co-precipitation mechanism and the finer scale β' carbide precipitates by a similar mechanism to that in the Fe-Si(C). The repeated precipitation on climbing dislocations is similar to earlier observations[6], and again points to the necessity of vacancies in the precipitation reactions.

Acknowledgements

This work was supported by the Director, Office of Energy Research, Office of Basic Energy Sciences, Division of Materials Sciences of the U.S. Department of Energy under Contract No W-7405-ENG-48. Dr. A. F. Rowcliffe is gratefully acknowledged for supplying the stainless steel samples.

References

1. R. F. Vyhnal and S. V. Radcliffe, Acta Met. 20, 435 (1972).
2. U. Dahmen, A. Pelton, M. J. Witcomb, and K. H. Westmacott, this conference proceedings.
3. U. Dahmen, K. H. Westmacott and M. J. Witcomb, this conference proceedings.
4. U. Dahmen, K. H. Westmacott and G. Thomas, Acta Met. 29, 627 (1981).
5. A. Pelton, 39th Ann. Proc. EMSA, Atlanta, GA 1981.
6. G. R. Kegg, J. M. Silcock and D. R. F. West, Metal. Sci. J. 8, 337 (1974).
7. A. F. Rowcliffe and B. L. Eyre, J. Phys. pt. F (Metal Phys.) 1, 771 (1971).
8. A. F. Rowcliffe and R. B. Nicholson, Acta Met. 20, 143 (1972).

Figure Captions

Fig. 1 {100} carbide precipitates in quenched Fe-Si(C), (a) aged 168 hrs. at 25°C, (b) aged 168 hrs. at 25°C plus 1 hr. at 100°C.

Fig. 2 Precipitation in quenched Fe-Cr-Ni(C,P), (a) aged 10 hrs. at 500°C, (b) aged 100 hrs. at 500°C.

Table 1

Nominal Composition (wt%)	Solution Treatment	Aging Treatment
Fe-2Si-0.15C	850°C 1hr	25°C 168hr
		25°C 168hr + 100°C 1hr
Fe-18Cr-10Ni-0.3P-0.01C	1150°C 1hr	500°C 10hr
		500°C 100hr

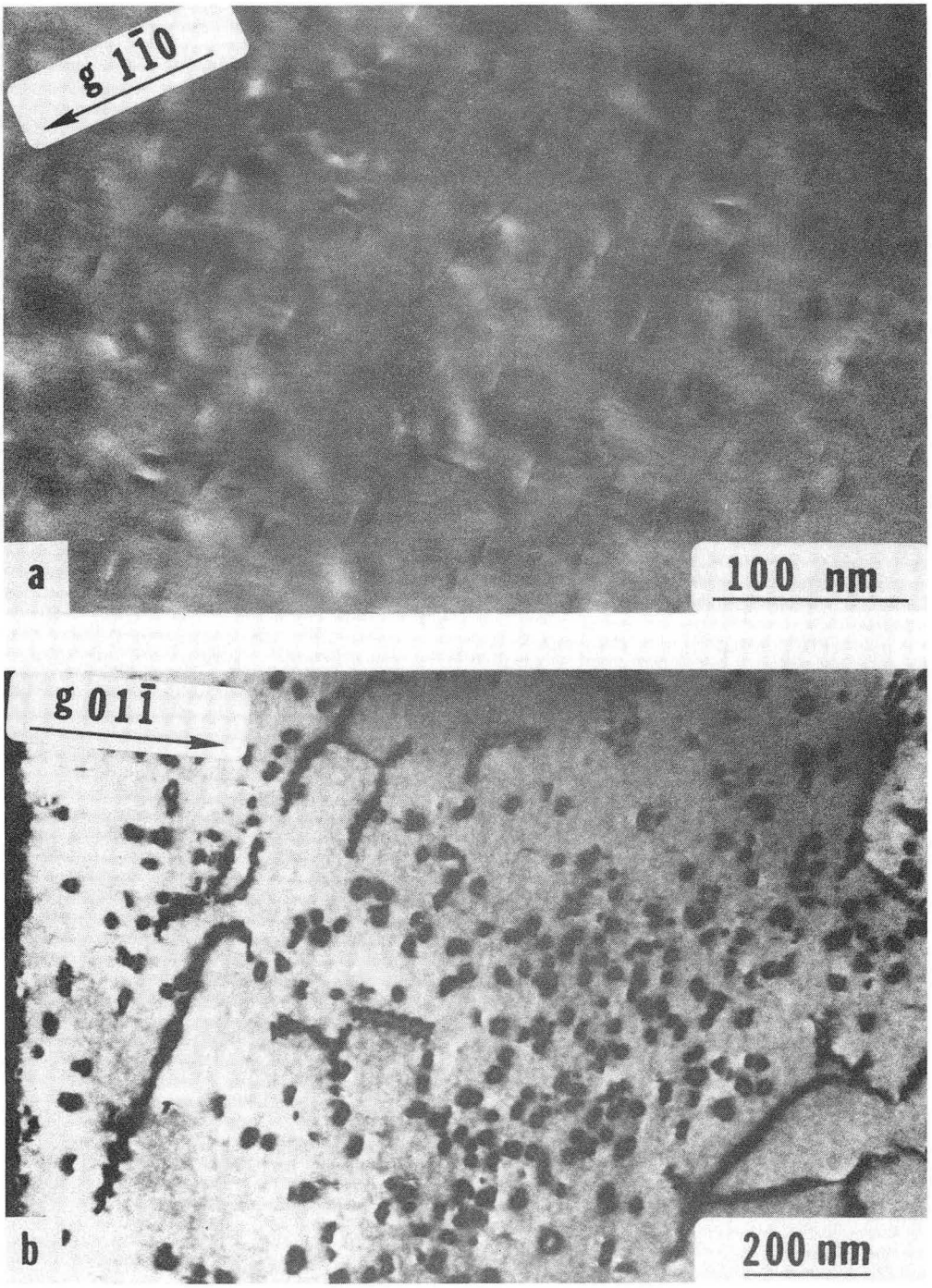

XBB 819-8423

Fig. 1

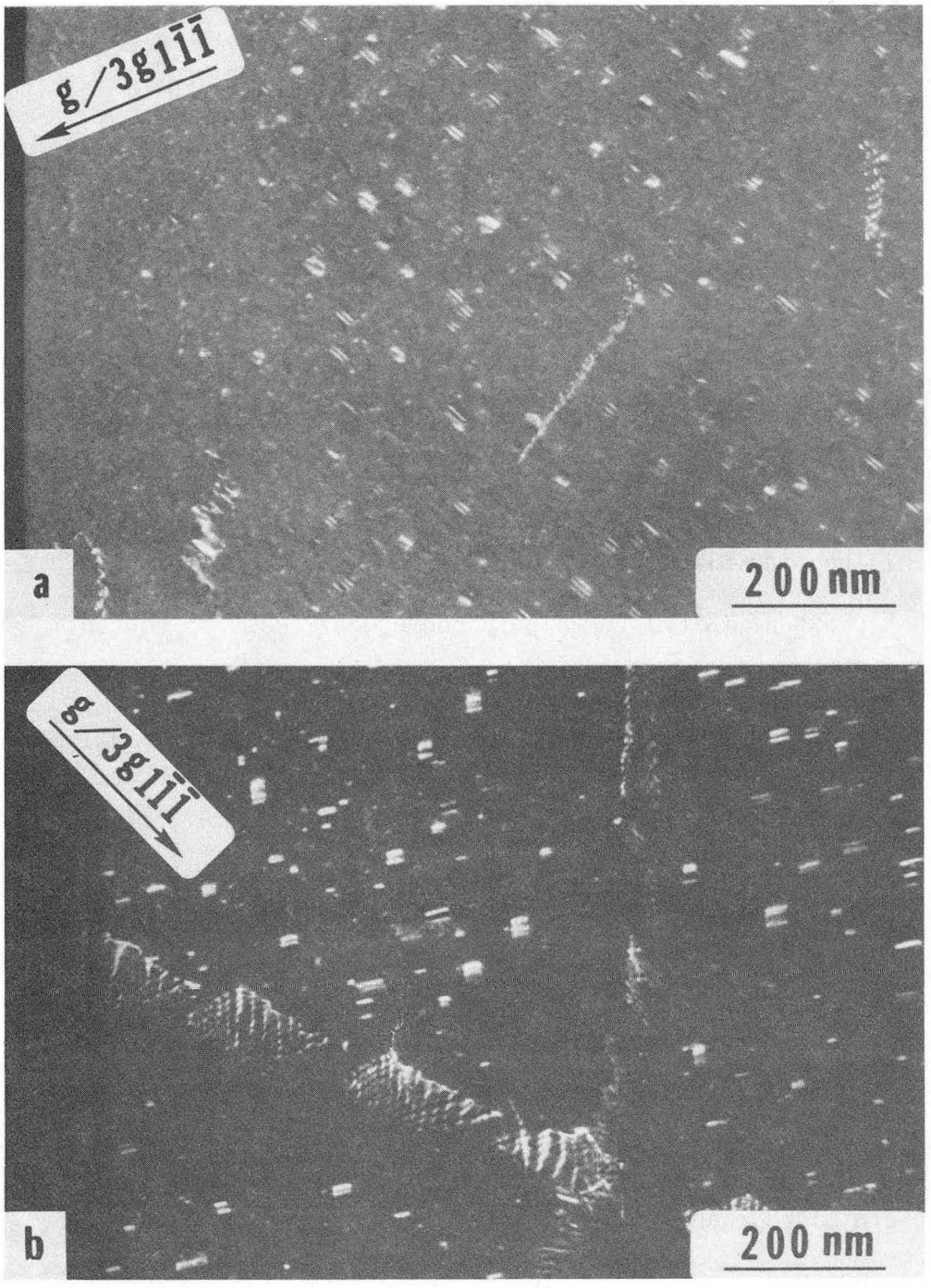

XBB 819-8422

Fig. 2

PAPER III

Techniques for the structural characterisation of precipitates by TEM are well-established. Large densities of small precipitates often form with plate morphology in the very earliest stages of alloy decomposition and these can be studied through the shape factor changes in the matrix diffraction pattern. At later stages, the structure and orientation relationship with the matrix of large individual precipitates may also be found by conventional electron diffraction techniques.

In recent years the minimum size at which structural information from discrete precipitates can be obtained has been greatly reduced by the use of the fine electron probes produced in Scanning Transmission Electron Microscope (STEM) (or highly convergent beams in conventional) instruments. However, the limiting conditions for the application of these microdiffraction techniques have not been fully explored. The present work concerns the characterisation of very thin plate precipitates in quenched and aged platinum containing small amounts (of the order of 880ppm) of residual carbon impurity.

Platinum strips were quenched from temperatures up to the melting point at pressures better than 4.5×10^{-6} Pa and then aged in air for various times at different temperatures. Electropolished samples were viewed at 100 kV in Philips EM400 and Siemens 102 microscopes. A typical bright field micrograph of a precipitate plate after a 773K aging treatment is shown in Figure 1. In Figure 2(a), a series of Convergent Beam Diffraction Patterns (CBDP's) obtained from such a plate by large angle tilting operations in a goniometer stage is reproduced. All the low order zone areas were recorded in turn to probe fully reciprocal space and characterise the precipitate structure. The faint precipitate spots and

and streaks interspersed with the matrix spots were observed only when the focused spot was centered on the precipitate and long exposure times were used. Patterns taken from the matrix adjacent to the precipitate showed only spots characteristic of the pure Pt fcc structure.

The reciprocal lattice model for the precipitate was reconstructed from the information contained in the reciprocal lattice sections such as Figure 2 and the resulting structure and its relation to the Pt matrix is illustrated in Figure 3. It is evident that the streaking of the precipitate spots results in an uncertainty of their positions. Best fit with the microdiffraction patterns was obtained for the face centered tetragonal cell shown in Figure 3 with a c axis of nearly 2/3 of the reciprocal lattice cell of the matrix. Since studies of the progressive development of the precipitates together with conventional contrast analysis indicated the plates were still quite thin, the lattice fringe image technique was employed to establish directly the precipitate thickness. An example of such an image from a precipitate intersected by both foil surfaces is shown in Figure 4. A series of lattice images were recorded along the length of the precipitate and several different plates were examined. In each case, the micrographs indicated a precipitate thickness in the [001] direction of about seven {200} layers. Laser optical diffraction patterns were obtained from the fringes and microdensitometer traces taken to compare the matrix and the precipitate {200} lattice spacing. Both sets of data showed an expansion of the lattice in the precipitate of $\sim$14-17%. All the observations are therefore self-consistent and show a precipitate structure with a {200} spacing 1/7th larger than the Pt lattice.

ACKNOWLEDGEMENTS

This work was supported by the Director, Office of Energy Research, Office of Basic Energy Sciences, Material Science Division of the U.S. Department of Energy under Contract No. W-7405-ENG-48. M. J. Witcomb gratefully acknowledges financial support from the Council of the University of the Witwatersrand, the C.S.I.R., Pretoria, and L.B.L.U.C.

FIGURE CAPTIONS

Fig. 1. a/3<100> faulted loops quenched from 1523K, aged 10h 773K.

Fig. 2. Precipitate convergent beam diffraction patterns.

Fig. 3. Reciprocal lattice model of precipitate.

Fig. 4. {002} lattice image of a seven layer precipitate (P).

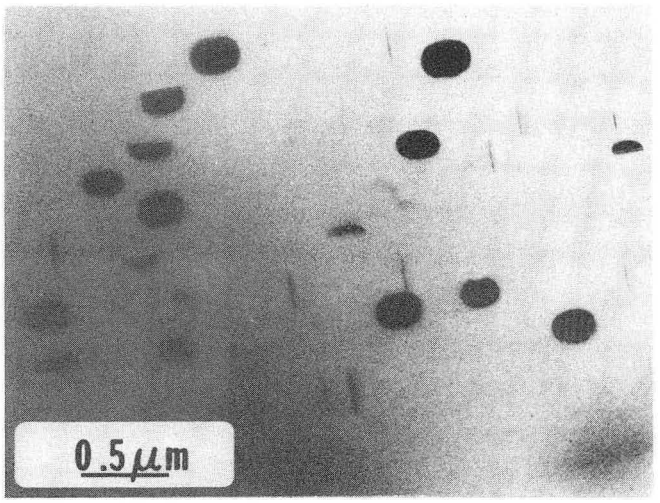

Fig. 1

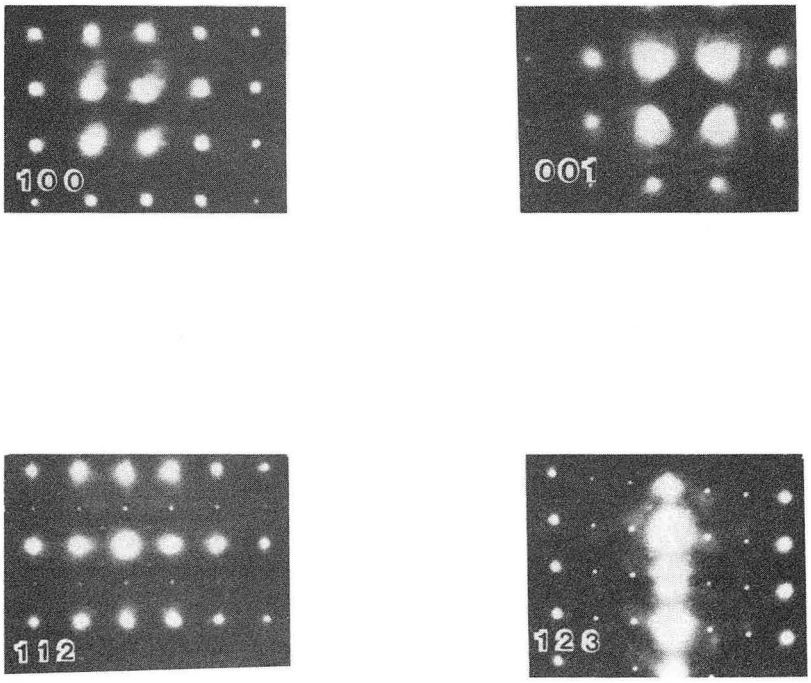

XBB 819-8428

Fig. 2

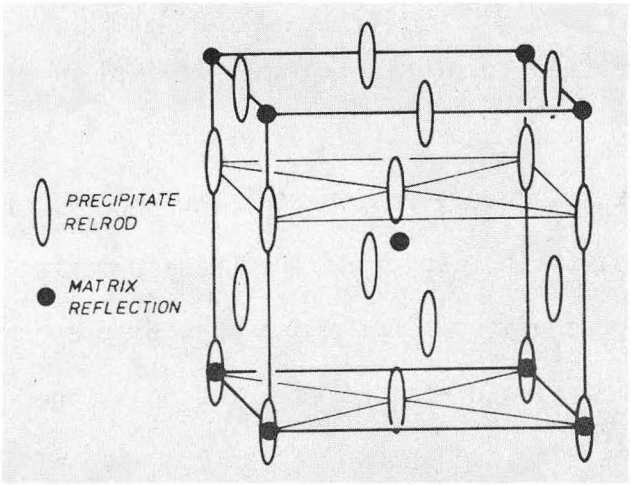

Fig. 3

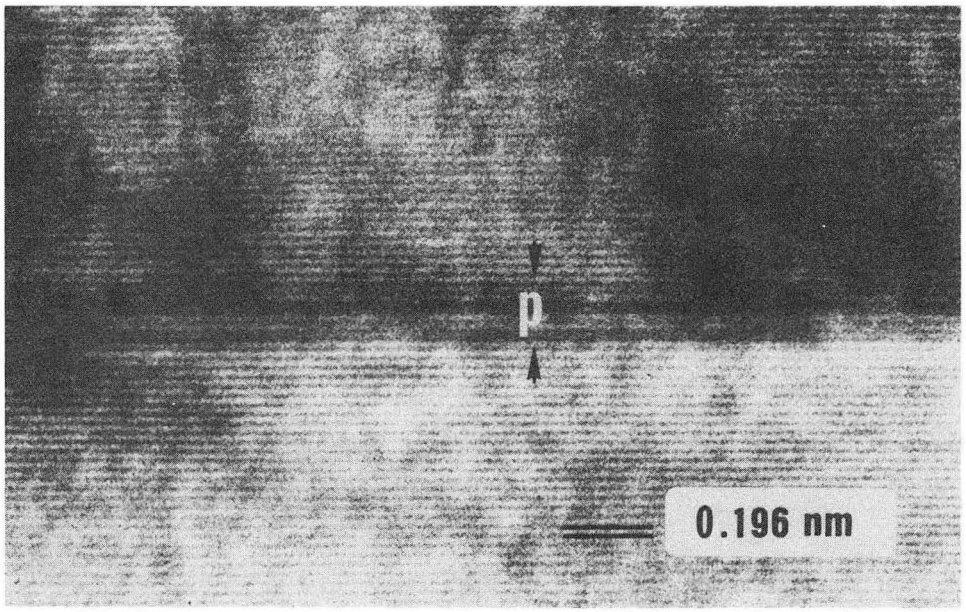

XBB 819-8421

Fig. 4

Paper IV

The concept of the invariant line is used to unify three previously diverse approaches to predicting the habit plane and orientation relationship in solid state phase transformations, namely, Eshelby's continuum theory, O-lattice theory, and martensite theory. Each of these theories addresses a different aspect of the transformation but each predicts minimum energy configurations which when displayed on appropriate plots share the common feature of poles lying on a cone. It is shown here that the underlying connection is the presence of an invariant line lying parallel to the product/parent habit plane.

A detailed crystallographic theory based on this concept is then outlined and compared with precise data recently reported for the Cu-Cr and Cu-Zn alloy systems. In both cases the predictions of the theory and results of the experiments are in excellent accord.

Introduction

The problem of predicting the shape and orientation of a precipitate in a solid-solid phase transformation has been approached in many different ways. Three approaches have been particularly successful: Eshelby's continuum theory for coherent elastic inclusions[1], the crystallographic theory of martensite transformations[2], and Bollmann's O-lattice theory[3]. Although based on completely different ideas, the three theories have much more in common than has been previously recognized. This may be illustrated with the stereograms in Figure 1 which apply to the common case of an fcc → bcc phase transformation described by the Bain distortion.

Figure 1(a) shows a "minimum energy trough" (shaded area) as calculated by Easterling and Thölen[4] on the basis of Eshelby's theory. They found the

strain energy of coherent plate-shaped inclusions to be a minimum when the habit plane normal was in the shaded area of the stereogram. Figure 1(b) shows the result of a calculation by two French groups[5,6] based on O-lattice theory. Using a second order approximation, they found that the orientations of optimum fit between an fcc and a bcc lattice have O-lines lying on a hyperboloid of revolution. Figure 1(c) shows the cones of unextended lines familiar from martensite theory.

The striking similarity of these three plots points to a common factor in the theories. This factor has recently been shown to be the invariant line[7]. In the theory of martensitic transformations, the invariant line is a familiar concept. Any vector on the cone of unextended lines (Figure 1(c)) may be rotated back to the position it had before the transformation. Another such vector is produced by a suitable lattice-invariant shear. Together, these two invariant lines define an invariant plane--the habit plane. This procedure ensures that the plane of contact between parent and product is macroscopically undistorted and mobile, as experimentally observed. The relative position of the two lattices (orientation relationship) and the habit plane are directly related to the crystallographic choice of shear system.

O-lattice theory considers a very similar problem: the optimum match of two crystal lattices across an interface. This interface can be a complicated surface or simply a plane, as in martensite theory. However, it does not have to be mobile or macroscopically distortion-free. Instead, it is now required that the interface contains a minimum of dislocations. This is the case when the O-lattice cell is maximized. A local maximum is achieved when one cell dimension goes to infinity and the O-lattice becomes

a line lattice. The interface then contains an invariant line and only one set of dislocations. This is the condition calculated by the French groups[5,6] and can be expressed in terms of Figure 1(b). The optimum interface plane will contain a vector on the cone of unextended lines. The particular choice of invariant line from all the vectors on the cone of unextended lines is dictated by the "efficiency" with which the available dislocations take up the transformation strain, and has been calculated by minimizing an "energy parameter" with the aid of a computer program[8].

Eshelby's theory of coherent elastic inclusions is formulated in terms of an elastic continuum, without direct reference to crystallography. Furthermore, it is strictly valid only for small strains. The minimum energy habit plane is determined by the transformation strains and the elastic constants of the material. Figure 1(a) shows that the habit planes thus predicted contain an invariant line. When taking into account the elastic anisotropy, significant variations in the habit plane orientation are predicted but these are not confirmed by experiment. It has been suggested instead that a more important parameter is the stress-free strain which incorporates the orientation relationship between matrix and inclusion[9]. This reduces the problem to one of optimum matching in the habit plane similar to O-lattice and martensite theory. Thus it appears that the factor common to these different theories is the requirement of an invariant line in the interface. On this basis, a more detailed crystallographic theory of precipitation can be proposed.

Theory

The relationship between two phases can be described by a transformation

matrix whether the transformation is diffusion controlled or diffusionless. This matrix describes the change in dimension of some unit cell as it undergoes the matrix to precipitate structural transition. It relates two crystal lattices regardless of the chemical species that occupies the lattice sites. Compositional changes are thus only taken into account indirectly, through their effect on the crystal structure. This assumption is justified not only in the case of martensite and massive transformations, where compositional changes are negligible, but also when the effects of the structural change dominate the effects of the composition gradient. Any number of lattice correspondences may be chosen, but the most significant ones relate primitive cells, such as in the Bain correspondence, for which the transformation matrix describes the movement of all the lattice sites in the transformation. Lattice correspondences for non-primitive unit cells may require shuffles in addition to the homogeneous strain to complete the structural change. (This is the case, for example, in the bcc→ hcp transformation). There exists a special relationship between the different possible lattice correspondences, such as the small primitive cells shown solid and the large cells shown dashed in Figure 2(a). To generate one lattice correspondence from another, a fixed relative rotation of the two lattices is required. This rotation is determined only by the symmetries of the two lattices. It can be shown that any two lattice correspondences are related in two distinctly different ways. In Figure 2(a) the homogeneous lattice strain creating the open lattice from the solid one is decomposed into a pure deformation B which is the lattice strain for the first lattice correspondence (solid in Figure 2(a)) followed by a pure rotation R. The same situation can be described as a simple shear S followed by a pure deformation P of a different unit cell (outlined

in Figure 2(b)). This equivalence may be written as RB = PS (Eq. 1) and it can be shown that for rational orientation relationships (i.e. low-index directions coinciding) the simple shear S lies in the direction of a lattice translation, or Burgers vector, of the matrix lattice. The rotation R which describes the orientation relationship of the two phases is then determined by two requirements:

1) RB must be an invariant line strain. This first requirement was shown to be common to the three theories considered and is possible if one principal strain has a sign opposite to the other two.

2) The second requirement is crystallographic in nature and attempts to optimize the plastic accommodation of the shape change in the transformed region. When losing coherency, a growing precipitate may punch out dislocation loops. Loops with an edge component can only be created in pairs of opposite sign whereas a pure shear loop requires no counterpart. Hence the loss of coherency through the nucleation of a shear loop will be preferred. This requires that S in Eq. (1) lies near the direction of a Burgers vector, and hence determines the specific rotation axis for R.

The strength of the present treatment lies in its ability to generalize and unify the disparate features of previous approaches. Thus, it takes into account the volume and shape changes of a transforming inclusion, as in Eshelby's theory; it minimizes the dislocation density at the interface when the transformation strains are in the direction of an available Burgers vector, as in O-lattice theory; and it equates the overall transformation strain to an invariant line strain, as required for the homogeneous strain component in martensite theory.

Comparison with Experiments

The Cu-Cr system is a good test case for the present theory because some very thorough experimental data was published recently. In Cu-rich alloys the transformation is particularly straight forward since essentially pure Cr (bcc) precipitates in essentially pure Cu (fcc). Weatherly et al.[10] observed small precipitate needles with large coherency strain fields lying along irrational directions of the Cu matrix. Most of the needle axes concentrated near <651> or <761> directions (Figure 3(a)). After longer aging times, almost all needles had taken on this direction (Figure 3(b)). Figure 3(a) shows that essentially all precipitate needles were on the cones of unextended lines and hence are likely to have an invariant line in the interface. Furthermore, the loss of coherency by shear loop nucleation requires the invariant line to lie on the {111} Cu planes. Hence the precipitates should all lie in the directions of intersection between the cone of unextended lines and the {111} planes. Using the lattice parameters of Cu and Cr at the aging temperaure, this is calculated to be a $<6.3, \overline{5.2}, \overline{1}>$ direction, in perfect agreement with the observations. The corresponding orientation relationship is within one degree of Kurdjumov-Sachs, also matching the experiments.

Cu-Zn in the range of 60 w/o Zn has the same ratio of lattice parameters as Cu-Cr, but the precipitate and matrix structures are interchanged, i.e. fcc precipitates in a bcc matrix. For optimum position during the loss of coherency, the precipitates should now lie along invariant lines in the {110} matrix planes. This was indeed observed by Crosky et al.[11] who discovered that surface precipitates also follow invariant lines whose specific directions are determined by the crystallographic indices of the

surface.

ACKNOWLEDGEMENTS

This work was supported by the Director, Office of Energy Research, Office of Basic Energy Sciences, Materials Science Division of the U.S. Department of Energy under Contract No. W-7405-ENG-48.

REFERENCES

1. J. W. Eshelby, Proc. Roy. Soc. (A) 341, 376 (1957).
2. C. M. Wayman, Introduction to the Crystallography of Martensitic Transformations, MacMillan, N. Y. (1964).
3. W. Bollmann, Crystal Defects and Crystalline Interfaces, Springer, N. Y. (1970).
4. K. E. Easterling and A. R. Thölen, Acta. Met. 24, 333 (1976).
5. R. Bonnet and F. Durant, Mat. Res. Bull. 7, 1045 (1972).
6. A. Perio, J. J. Bacmann, M. Suery and A. Eberhardt, Revue de Phys. Appl. 1197 (1977).
7. U. Dahmen, Acta. Met., in press.
8. W. Bollmann and H. U. Nissen, Acta Cryst. A24, 546 (1968).
9. U. Dahmen, K. H. Westmacott and G. Thomas, Acta Met. 29, 627 (1981).
10. C. G. Weatherly, P. Humble and D. Borland, Acta Met. 27, 1815 (1979).
11. A. Crosky, P. G. McDougall and J. S. Bowles, Acta Met. 28, 1495 (1980).

FIGURE CAPTIONS

Fig. 1. Stereograms showing the habit planes in an fcc → bcc transformation predicted by: a) the theory of elastic coherent inclusions[4], b) O-lattice theory[5,6] and c) martensite theory[2].

Fig. 2. Two different decompositions of the strain creating the open lattice from the solid lattice: a) a strain B followed by a rotation R, b) a simple shear S followed by a strain P. Lattice correspondences are depicted by solid unit cells.

Fig. 3a. Stereogram showing the distribution of coherent Cr needles in Cu[10] with cones of unextended lines.

Fig. 3b. Clustering of the needle directions during growth[10] as required for the nucleation of shear loops.

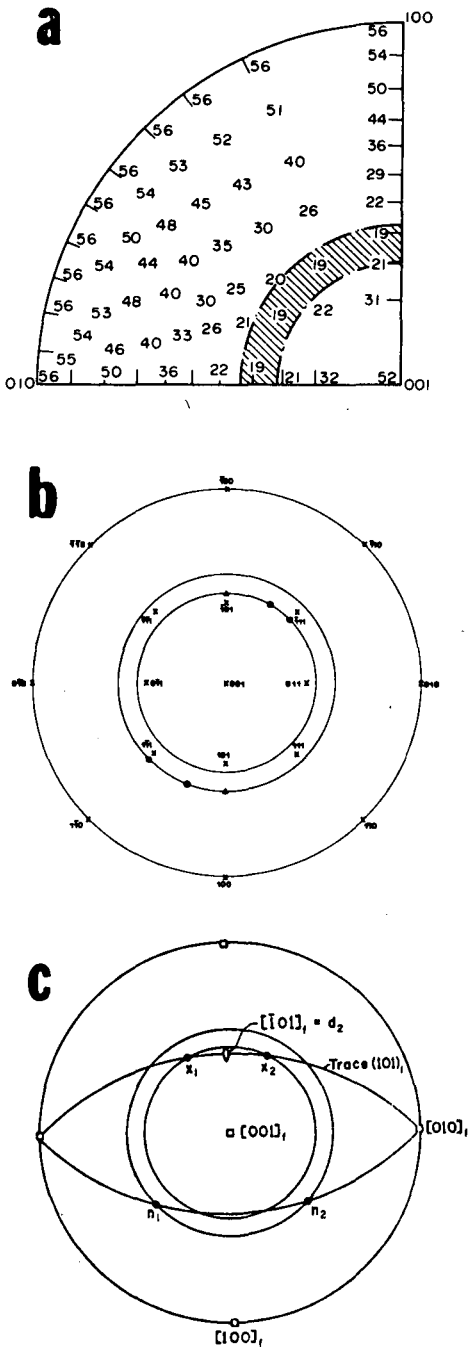

XBL 817-10885A

Fig. 1

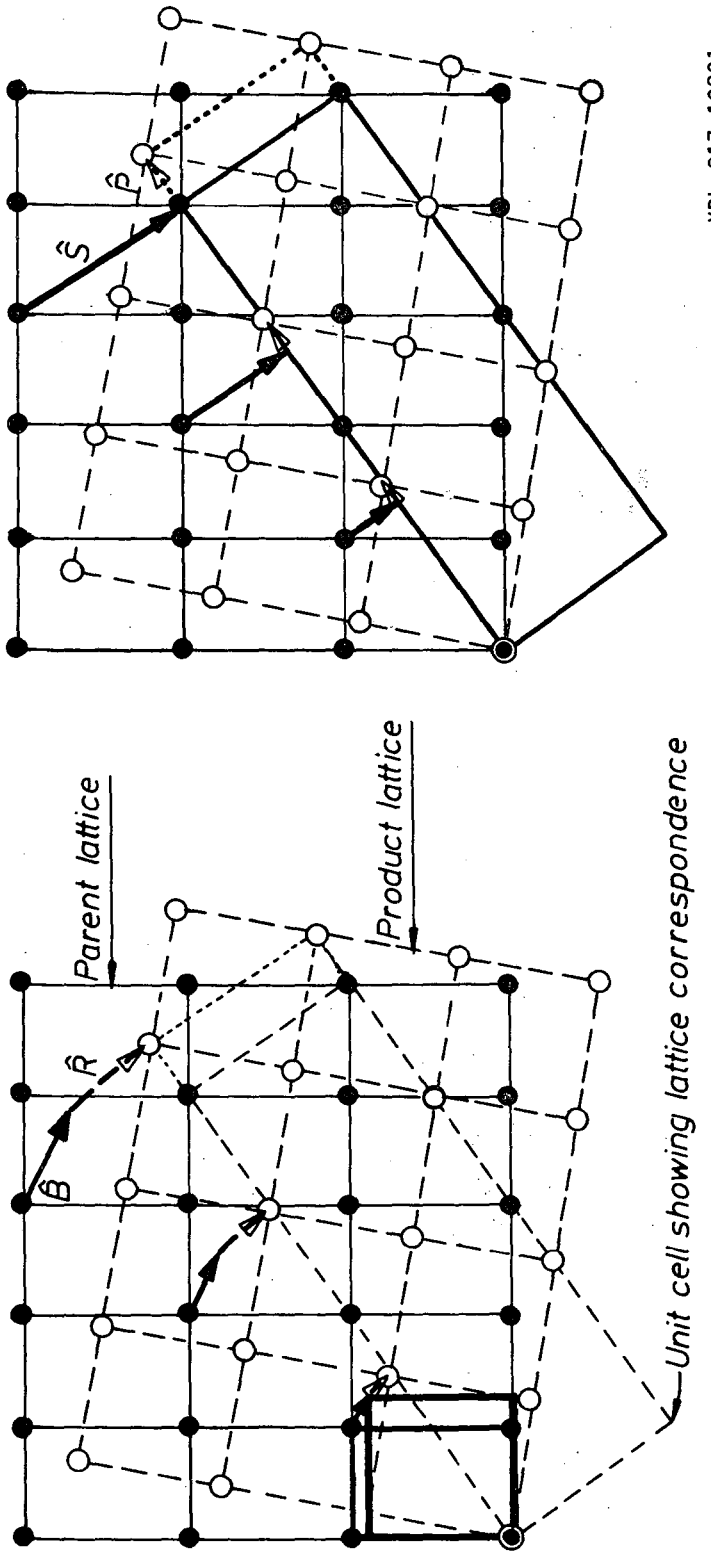

XBL 817-10891

Fig. 2

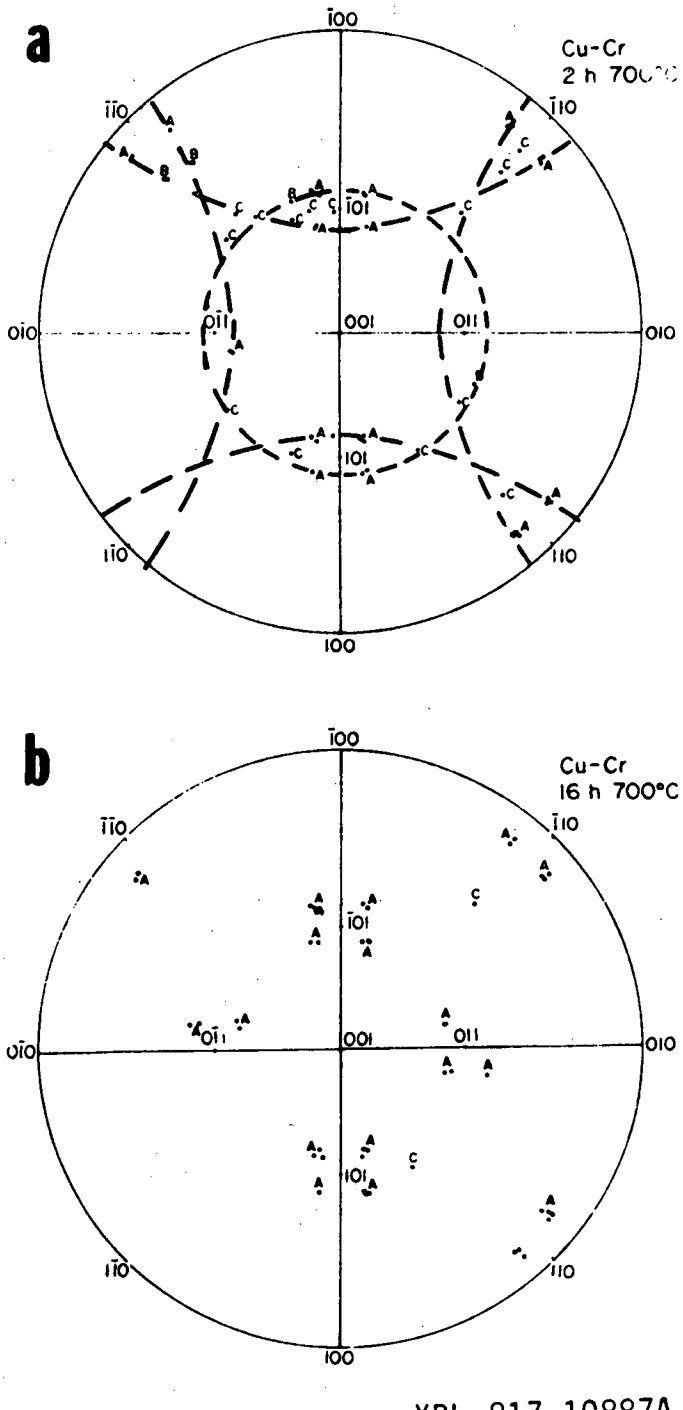
a
Cu-Cr
2 h 700°C
b
Cu-Cr
16 h 700°C
100
110
010
001
011
101
XBL 817-10887A

Fig. 3

PAPER V

The importance of quenched-in vacancies in the precipitation of a second phase from a supersaturated solid solution has long been recognized and three separate but related effects identified: (i) the increased diffusivity of solute atoms in a vacancy supersaturation; (ii) the possible role of vacancies in zone formation[1]; and (iii) the volume effect of vacancies on the formation of a critical size nucleus[2,3]. However, the detailed mechanisms by which vacancies could play a structural role in precipitate formation have not been extensively studied. Recent results on interstitial alloys suggest that this aspect may be much more important than previously recognized. In this paper a simple model is outlined which incorporates accepted ideas and is capable of explaining the observed structures in widely diverse alloy systems.

Model

It is well-established from both theoretical and experimental work that vacancies and solute atoms in a terminal solid solution may interact and associate. It is not surprising therefore that when both are present in supersaturation, their ultimate fates are closely interconnected. In predicting this fate several important parameters must be considered: the solute concentration c_s (assumed to be in the range $0\text{-}10^{-2}$); the vacancy concentration c_v (10^{-5} - 10^{-3}); the concentration and binding energy of solute/vacancy pairs, c_p and E_b; and their respective mobilities. Even in simple binary alloys a wide range of behavior is possible with changes in the value of these parameters. This is more evident still if the effects of temperature on the partitioning of vacancies between the bound and free states, the competing processes of secondary defect

formation and solute-clustering, and the dynamic equilibrium between free and bound vacancies during such clustering processes are also taken into account. Clearly, the complexity of the situation permits only extreme cases to be analysed. Thus in this note we consider (i) interstitial solutions where a large positive misfit results in a strongly bound solute atom/vacancy pair which migrates significantly faster than a free vacancy; (ii) substitutional systems where E_B is smaller and the complex migrates significantly slower than free vacancies. This is followed by a brief discussion of the mechanism of vacancy-assisted precipitate formation.

When considering the nucleation of precipitates by the clustering of complexes, two possibilities are evident: (i) the vacancies are dispersed in the precipitate and serve the function of accommodating excess precipitate volume; or (ii) the complexes condense in a planar configuration giving rise to a plate-shaped precipitate bounded by a dislocation loop, i.e. a semicoherent precipitate forms. With this background, various possibilities for different types of alloy systems will now be compared with observations.

Case I - Interstitial Solutions

Interstitial solute atom solubilities in the FCC metals are usually of the same order as the equilibrium vacancy concentration at the melting point (10^{-3} to 10^{-4}) and significant effects of impurities on vacancy clustering are found[4]. In extreme cases, e.g. the reactive metals, Cu, Ag and Ni, the formation of dislocation loops is completely suppressed. In the case of carbon in Pt, the large C-V binding energy leads to the association of all the carbon with vacancies at low temperatures following

a quench, and co-precipitation of the complexes on {001} planes[5], Figure 1. Samples quenched from the melting point contain a high density of precipitate plates, whereas samples given a post-quench age at 400°C contain both the precipitates and a high density of voids. When the quench temperature is reduced to 1250°C, only precipitate structures are found following a quench or quench and age. These results suggest a sequence of events in which (a) vacancies and solute atom associate during the quench, (b) the resulting complexes cluster and (c) the remaining free vacancies form voids during the postquench age (∿400°C).

In BCC metals the larger solubilities for interstitials leads to a somewhat different situation. The absence of secondary defect structures in nominally pure BCC metals may be due to a large E^F/E^M ratio leading to large vacancy losses during the quench, or to the inhibiting effects of residual impurities, as in FCC Cu, Ni and Ag. On the other hand when significant amounts of C, O or N are present, all the vacancies become paired with solute atoms and analogous structures to those observed in Pt(C) are found. For example, a study of the Ta(C) system has provided evidence that the earliest stages of precipitation involve vacancy participation [6]. Figure 2 shows a quenched and aged Ta-0.5%C specimen which contains a precipitate denuded zone at the grain boundary due to vacancy depletion. Further striking evidence that precipitate growth requires a continuing supply of vacancies was found in an austenitic Fe-Ni-Cr-P alloy[7]. After quenching this steel from 1150°C and aging at 500°C, a fine dispersion of precipitates was observed in the matrix and on dislocations together with larger vacancy-type plate defects also in the matrix. After a further long age at 600°C, further precipitation

had occurred on the dislocation as it climbed and supplied vacancies whereas no change was found in the size of the matrix precipitates.

Case II - Substitutional Solutions

In FCC substitutional alloys the balance between precipitate and dislocation loop formation becomes delicate and depends sensitively on the value of E_b. Moreover, other factors such as the metastable phase boundaries for the precipitating phase and dislocation loops can become important. If the vacancy mobility is much greater than that of the complex, then loops can nucleate and will continue to grow as the dynamic equilibrium between bound and free vacancies provides a continuing supply of vacancies. Precipitation will then be delayed until the temperature range where loop shrinkage again supplies vacancies. This behavior is found in Al-Si alloys as illustrated in Figure 3. In the quenched plus 100°C aged condition, only dislocation loops are observed (Figure 3(a)). However, during in-situ annealing at 150°C, a fine precipitate structure is observed to emerge as the loops shrink (Figure 3(b)). This phenomenon is found only in thicker regions of the foil where the vacancies have not entirely escaped to the foil surfaces. The necessity for vacancies is further stressed by the developing precipitate-free zones along grain boundaries such as at A in Figure 4. Even though their formation clearly involves vacancies, the precipitates have interstitial character. These characteristics parallel those found in the Ta(C) system.

Al-Mg alloys provide an example where both loop formation and precipitation occur in the same temperature range, as illustrated in Figure 5. A fine scale precipitate structure is interspersed

with precipitate-free regions which contain large perfect prismatic dislocation loops. These structures have been observed and discussed in these terms previously[8]. Lack of space limits further discussion, but many examples of similar effects in BCC substitutional alloys, e.g. Fe-Mo, Fe-Au, may be cited[9].

Discussion

The central feature in each case is the association of vacancies with oversize solute atoms. During precipitation the vacancies participate in the nucleation event in a cooperative manner as a semi-coherent precipitate forms. Subsequent growth is then facilitated. Perhaps the simplest way to view this process is to compare it with the loss of coherency of a precipitate by a loop punching mechanism as illustrated in Figure 6. During the growth of a slightly oversize coherent precipitate, the accumulating stress is eventually relieved by the formation of a pair of prismatic dislocation loops of opposite sign. The anticoherency dislocation remains in the interface, while the other loop is punched in the matrix. In the co-precipitation mechanism, the disparity between the precipitate and matrix structure is so great that the misfit dislocation loop must be formed at the outset to allow the precipitate to nucleate and grow, i.e. Step 3 of Figure 6 without the matrix loop. The implications of this conclusion are that in the cases where co-precipitation occurs the true precipitate structure is established during nucleation and strong evidence for this has been found in the Ta(C) study[6]. The volume misfit of the precipitating phase in its equilibrium crystal structure seems to be directly related to the precipitate habit plane. Below 30% misfit the habit plane in a BCC matrix

is {013}, e.g. Ta(Ta_2C), V(V_2C), Nb(Nb_2C), Mo(TiN), Mo(TiC), and above 40% an {001} habit is found, e.g. Mo(HfN), Mo(HfC), Mo(ZrN), Mo(ZrC)[10], Fe(V_4C_3). In other interstitial [Pt(C), Fe-Si(C), Fe-Ni-Cr(P), Fe(N)] and substitutional systems (Al-Mg, Al-Au. Fe-Mo, Fe-Au, Cu-Ag) {001} habit planes are observed whereas {111} (in Al-Si) and {013} (in Al-Mg) are much less common. The solute atom misfit for these systems ranges from 10 to 60% and it appears that in most cases, the observed precipitate habit is associated with optimum use of the vacancies in forming and accommodating the new crystal structure.

Acknowledgement

This work was supported by the Director, Office of Energy Research, Office of Basic Energy Sciences, Materials Science Division of the U.S. Department of Energy under Contract No. W-7405-ENG-48, and a grant from the Science Research Council of South Africa.

References

1. L. A. Girifalco and H. Herman, Acta Met. 13, 583 (1965).
2. K. C. Russell, Scripta Met. 3, 313 (1969).
3. A. G. Khachaturyan, Sov. Phys.-Solid State 13, 2024 (1972).
4. K. H. Westmacott, Cryst. Lattice Defects 6, 203 (1976).
5. U. Dahmen, M. J. Witcomb and K. H. Westmacott, this conference proceedings.
6. U. Dahmen, K. H. Westmacott and G. Thomas, Acta Met. 29, 627 (1981).
7. A. Pelton and K. H. Westmacott, this conference proceedings.
8. A. Eikum and G. Thomas, Acta Met. 12, 537 (1964).
9. E. Hornbogen, G. R. Speich and J. B. Clark, eds. Precipitation from Iron Based Alloys, p. 1, Gordon Breach, N. Y. 1965.
10. N. E. Ryan, W. A. Soffa and R. Crawford, Metallography 1, 195 (1968).

Figure Captions

Fig. 1. Carbon-vacancy precipitates on {001} planes in quenched Pt.

Fig. 2. Precipitate-free zone at grain boundary in quenched Ta-0.5%C alloy.

Fig. 3. Al-1 w/o Si alloy showing a) vacancy loops after quenching, b) the same area after annealing 10 min at 105°C. The loops have shrunk, unfaulted and fine precipitates are forming.

Fig. 4. Precipitate-free zone in a quenched Al-1 w/o Si alloy after in-situ annealing at 150°C.

Fig. 5. Al-7 w/o Mg alloy showing absence of precipitates near dislocation loops.

Fig. 6. Schematic of a growing precipitate losing coherency by prismatic loop punching.

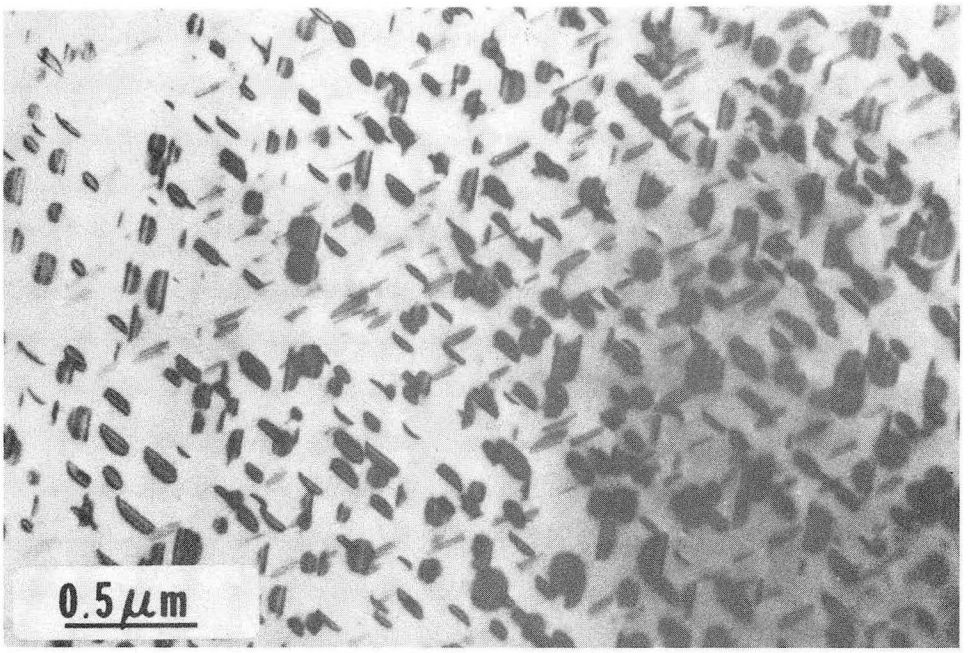

Fig. 1

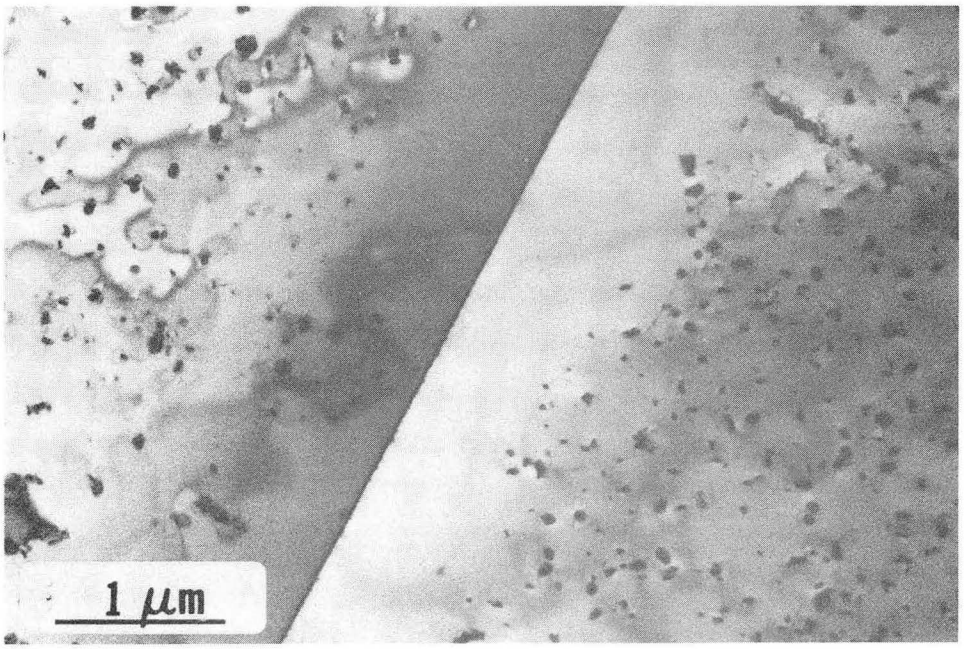

XBB 819-8424

Fig. 2

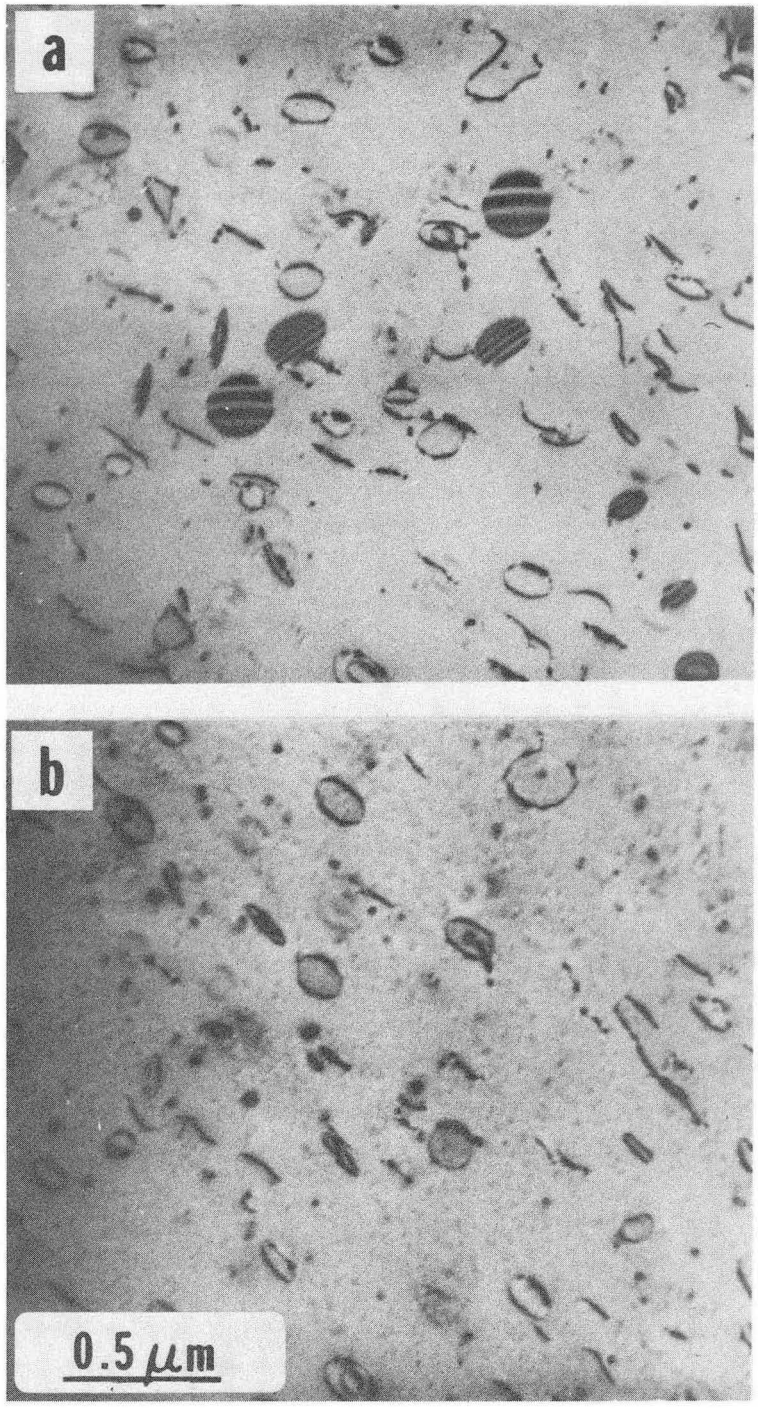

XBB 819-8426

Fig. 3

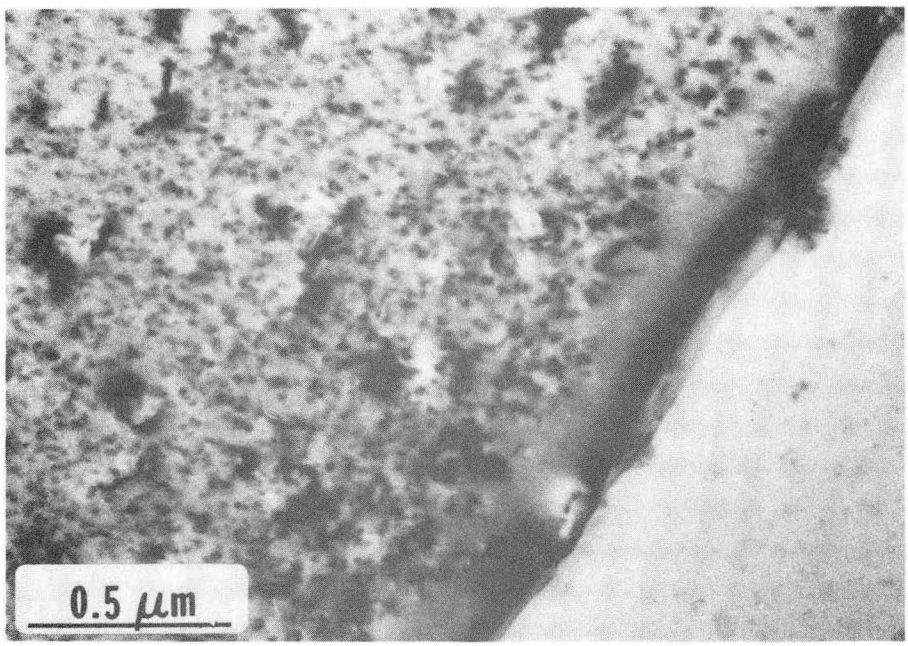

Fig. 4

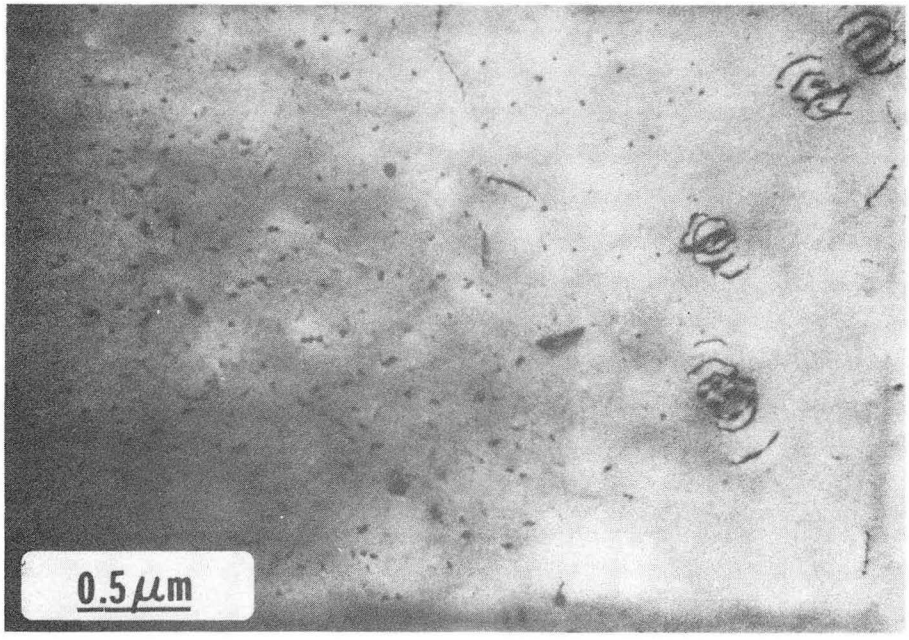

XBB 819-8425

Fig. 5

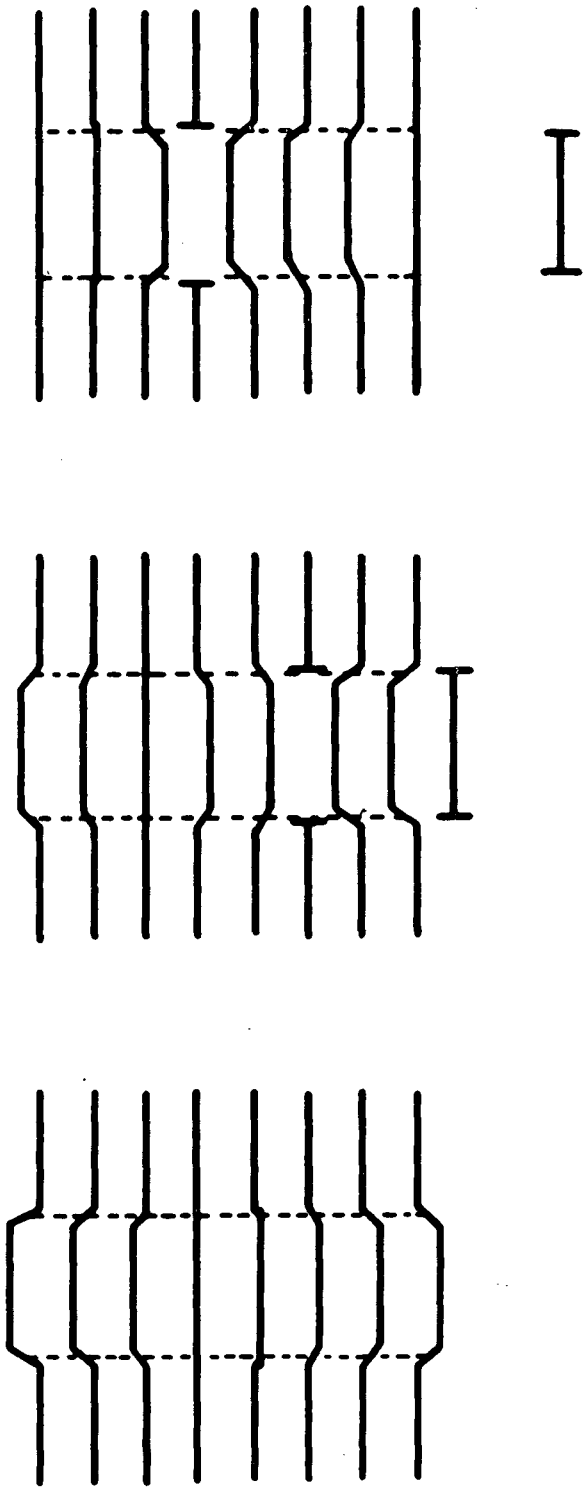

XBL 817-10890

Fig. 6

This report was done with support from the Department of Energy. Any conclusions or opinions expressed in this report represent solely those of the author(s) and not necessarily those of The Regents of the University of California, the Lawrence Berkeley Laboratory or the Department of Energy.

Reference to a company or product name does not imply approval or recommendation of the product by the University of California or the U.S. Department of Energy to the exclusion of others that may be suitable.

TECHNICAL INFORMATION DEPARTMENT
LAWRENCE BERKELEY LABORATORY
UNIVERSITY OF CALIFORNIA
BERKELEY, CALIFORNIA 94720